Extinguishment and Enhancement of Propane Cup-Burner Flames by Halon and Alternative Agents

Takahashi, F.[1]*, Katta, V. R.[2], Linteris, G. T.[3], and Babushok, V. I.[3]

[1]Case Western Reserve University, Department of Mechanical & Aerospace Engineering, Cleveland, Ohio, USA.
[2]Innovative Scientific Solutions, Inc., Dayton, Ohio, USA.
[3]National Institute of Standards and Technology, Gaithersburg, Maryland, USA.
**Corresponding author email: fxt13@case.edu*

ABSTRACT

Computations of cup-burner flames in normal gravity have been performed using propane as the fuel, in addition to a propane-ethanol-water mixture studied previously, to reveal the combustion inhibition and enhancement by the CF_3Br (halon 1301) and potential alternative fire-extinguishing agents (C_2HF_5, $C_2HF_3Cl_2$, and $C_3H_2F_3Br$). The time-dependent, two-dimensional numerical code, which includes a detailed kinetic model (up to 241 species and 3918 reactions), diffusive transport, and a gray-gas radiation model, reveals a unique *two-zone* flame structure. For propane, general trends in the structure are similar to those of the fuel mixture. The peak reactivity spot (i.e., reaction kernel) at the flame base stabilizes a trailing flame, which is inclined inwardly by a buoyancy-induced entrainment flow. As the volume fraction of agent in the coflow increases gradually, the *premixed*-like reaction kernel weakens, thus inducing the flame base detachment from the burner rim and blowoff-type extinguishment eventually. The H_2O in the inner zone is converted further, primarily in the outer zone, to HF and CF_2O through exothermic reactions most significantly with the C_2HF_5 addition. Despite endothermic decomposition of the agent, exothermic reactions of the inhibitor fragments also contribute to the heat-release rate in the outer zone. Although the rates of formation (and associated heat-release rates) of HF and CF_2O are lower for propane, compared to the fuel mixture, two heat-release-rate peaks in the *two-zone* flame structure in the trailing flame are comparable for both fuels. A main heat-release step to form CO_2 in the hydrocarbon-O_2 combustion takes place in-between the two zones. The total heat release of the entire flame decreases (inhibiting) for CF_3Br but increases (enhancing) for the halon alternative agents, particularly C_2HF_5 and $C_2HF_3Cl_2$. Addition of C_2HF_5 resultes in unusual (non-chain branching) reactions and increases total heat release (combustion enhancement) primarily in the trailing *diffusion* flame.

KEYWORDS: Aircraft cargo-bay fire suppression, Diffusion flame stabilization, Halon 1301 replacement, Reaction kernel.

INTRODUCTION

In accordance with the Montreal Protocol to protect the stratospheric ozone layer, the use of the effective fire suppressant CF_3Br (bromotrifluromethane, Halon 1301) has been discontinued except for certain critical applications such as the suppression of cargo-bay fires in aircraft. Halon alternative agents must pass a mandated Federal Aviation Administration (FAA) test [1, 2], in which a simulated explosion of an aerosol can, caused by a fire, must be suppressed by the agent. Unlike CF_3Br, some replacement agents, including C_2HF_5 (pentafluoroethane, HFC-125) and $C_3H_2F_3Br$ (2-bromo-3,3,3-trifluoropropene, 2-BTP), when added at any concentration less than that required for inerting, created a higher over-pressure in the test chamber and thus failed the test.

Recent work [3-5] employing thermodynamic equilibrium and perfectly stirred-reactor calculations (for premixed systems) revealed that higher overpressures in the FAA aerosol can

Proc. of the Eighth International Seminar on Fire & Explosion Hazards (ISFEH8), pp. xx-xx
Edited by J. Chao, V. Molkov, P. Sunderland, F. Tamanini and J. Torero
Published by USTC Press
ISBN: xxx-xxx-xx-xxxx-x :: doi: xx.xxxx/xxx-xxx-xx-xxxx-x_0x-0x

tests might be due to higher heat release from reaction of the inhibitor itself. Nonetheless, the agents should still reduce the overall reaction rate and inhibit the reaction. For diffusion flames, however, the flame structure, combustion inhibition, and enhancement processes are not yet fully understood. In previous papers [6, 7], the authors reported the results of comprehensive numerical simulations for zero- and normal Earth-gravity cup-burner flames using the FAA aerosol can test [ACT] fuel mixture with CF_3Br, C_2HF_5, $C_2HF_3Cl_2$ (2,2-dichloro-1,1,1-trifluoroethane, HCFC-123), and $C_3H_2F_3Br$ added to the coflowing air. Additional numbers of carbon and fluorine atoms in the halon-replacement-agent molecules, compared to CF_3Br, represent potential energy contributions at a fixed concentration if they burn to COF_2 and HF. Nonetheless, the ACT fuel is somewhat unusual in that it contains a large portion of water (which is an important reactant with the halogenated species). The objectives of this study are to investigate the effects of fire-extinguishing agents (with different numbers of carbon and types of halogen) on the diffusion flame and to determine if the enhanced heat release found for the previous simulations with the ACT fuel occur with a more typical hydrocarbon fuel (propane).

COMPUTATIONAL METHOD

A time-dependent, axisymmetric numerical code (UNICORN) [18, 19] is used for the simulation of coflow diffusion flames stabilized on the cup burner. The code solves the axial and radial (z and r) full Navier-Stokes momentum equations, continuity equation, and enthalpy- and species-conservation equations on a staggered-grid system. A clustered mesh system is employed to trace the gradients in flow variables near the flame surface. The thermo-physical properties such as enthalpy, viscosity, thermal conductivity, and binary molecular diffusion of all of the species are calculated from the polynomial curve fits developed for the temperature range 300 K to 5000 K. Mixture viscosity and thermal conductivity are then estimated using the Wilke and Kee expressions, respectively. Molecular diffusion is assumed to be of the binary-diffusion type, and the diffusion velocity of a species is calculated using Fick's law and the effective-diffusion coefficient of that species in the mixture. A simple radiation model [20] based on the optically thin-media and gray-gas assumptions was incorporated into the energy equation. Radiation from CH_4, CO, CO_2, H_2O, HF, COF_2 and soot was considered in the present study. The Plank-mean absorption coefficients are obtained from the literature for the first four species [20] and HF [21]; or calculated for COF_2 [21] and soot [22]. The finite-difference forms of the momentum equations are obtained using an implicit QUICKEST scheme [18], and those of the species and energy equations are obtained using a hybrid scheme of upwind and central differencing.

A comprehensive reaction mechanism was assembled for the simulation of propane or ACT fuel flames with CF_3Br, C_2HF_5, $C_2HF_3Cl_2$, or $C_3H_2F_3Br$ added to air from four mechanisms: the four-carbon hydrocarbon mechanism of Wang and co-workers [23, 24] (111 species and 1566 one-way elementary reactions), detailed reactions of ethanol (5 species and 72 reactions) of Dryer and co-workers [25-27], the bromine and chlorine parts of the mechanism of Babushok et al. [28-31] (10 additional species and 148 reactions), and a subset (51 species and 1200 reactions) of the National Institute of Standards and Technology (NIST) HFC starting mechanism [32, 33]. The final chemical kinetics model (187 species, 3198 reactions for CF_3Br, C_2HF_5, and $C_3H_2F_3Br$; or 241 species and 3918 reactions for $C_2HF_3Cl_2$) and a soot model [22] are integrated into the UNICORN code. Transport data for 139 species are available in the literature; for the remaining 38 species, data are constructed by matching these species with the nearest species (based on molecular weight) with known transport data.

The ACT fuel is a propane-ethanol-water mixture [1, 2] with the volume fractions of the components: $X_{C_3H_8} = 0.159$, $X_{C_2H_5OH} = 0.454$, and $X_{H_2O} = 0.387$. Table 1 shows the minimum extinguishing concentrations (MECs) of fire-extinguishing agents for n-heptane and propane

fuels using the cup-burner method [8, 9] in the literature [8-16]. The calculated MEC obtained in this study are also listed and discussed in the results section.

Table 1. Measured and calculated minimum extinguishing concentrations.

Agent	Chemical	Formula	Measured n-Heptane MEC (%)	Measured Propane MEC (%)	Calculated ACT Fuel MEC (%)	Calculated Propane MEC (%)
Halon 1301	Bromotrifluromethane	CF_3Br	3.0 to 3.2 [10-12]	3.8 to 4.3 [11,13,14]	2.26	2.64
HFC-125	Pentafluoroethane	C_2HF_5	8.7 to 9.3 [8-12]	10.2 to10.4 [11,13]	8.40	7.65
HCFC-123	2,2-dichloro-1,1,1-Trifluoroethane	$C_2HF_3Cl_2$	7.1 to7.4 [15]	N/A	(4.90[b])	(4.60[b])
2-BTP	2-bromo-3,3,3-Trifluoropropene	$C_3H_2F_3Br$	2.6 [16] 4.7 [17][a]	N/A	(1.87[b])	(2.50[b])

[a]The fuel temperature: 50 °C.
[b]A concentration above which the calculation was unable to obtain the solution.

The boundary conditions are treated in the same way as reported in earlier papers [6, 7]. The computational domain is bounded by the axis of symmetry, a chimney wall, and the inflow and outflow boundaries. The burner outer diameter is 28 mm and the chimney inner diameter is 95 mm. The burner wall (4-mm long and 1-mm thick tube) temperature is set at 600 K and the wall surface is under the no-slip velocity condition. The mean fuel velocities for the ACT fuel and propane are 0.853 cm/s and 0.307 cm/s, respectively, and the mean velocity of the oxidizer ("air" [21 % O_2 in nitrogen] with added agent) is 10.7 cm/s at 294 K.

Validation of the code with the kinetic model was performed through the simulation of opposing-jet diffusion flames. The predicted extinction strain rates for propane-air flames (no agent) were within 7.5% of the measured values (with an error margin of 9 %) by Zegers et al. [34]. The predicted extinction agent concentrations for CF_3Br and C_2HF_5 are within 4 % of the measured concentrations in weakly stretched flames and within 25 % in highly stretched flames. Although cup-burner data using the ACT fuel are unavailable for a direct comparison, computation with the assembled reaction mechanism should provide insights into the detailed flame structure.

RESULTS AND DISCUSSION

The flame base supports a trailing flame and controls the flame attachment, detachment, and oscillation processes [35, 36]. Small variations in the agent volume fraction in the coflowing oxidizing stream (X_a) results in profound changes near the extinguishment limit. Figure 1 shows the calculated structure of near-limit propane flames in air with added agent: (a) CF_3Br, X_a=0.0258; (b) C_2HF_5, X_a=0.0765; (c) $C_2HF_3Cl_2$, X_a=0.0455; and (d) $C_3H_2F_3Br$, X_a=0.0246. The variables include the velocity vectors (**v**), isotherms (T), and heat-release rate ($\dot{q}$). The base of the agent-added flames are detached and drift inward a few mm away from the burner rim by the nearly horizontal entrainment flow. In contrast to zero-gravity ($0g_n$) flames [6], which are formed vertically, the normal gravity ($1g_n$) flame inclines inwardly due to the streamline shrinkage in the accelerating buoyancy-induced flow. The contours of the heat-release rate show a peak reactivity spot (i.e., the *reaction kernel* [35]) at a height from the burner rim, z_k = 0.8 mm to 1.8 mm. The chain radical species (H, O, and OH) as well as heat diffuse back against the oxygen-rich flow at the flame base (edge), thus promoting vigorous reactions to form the reaction kernel.

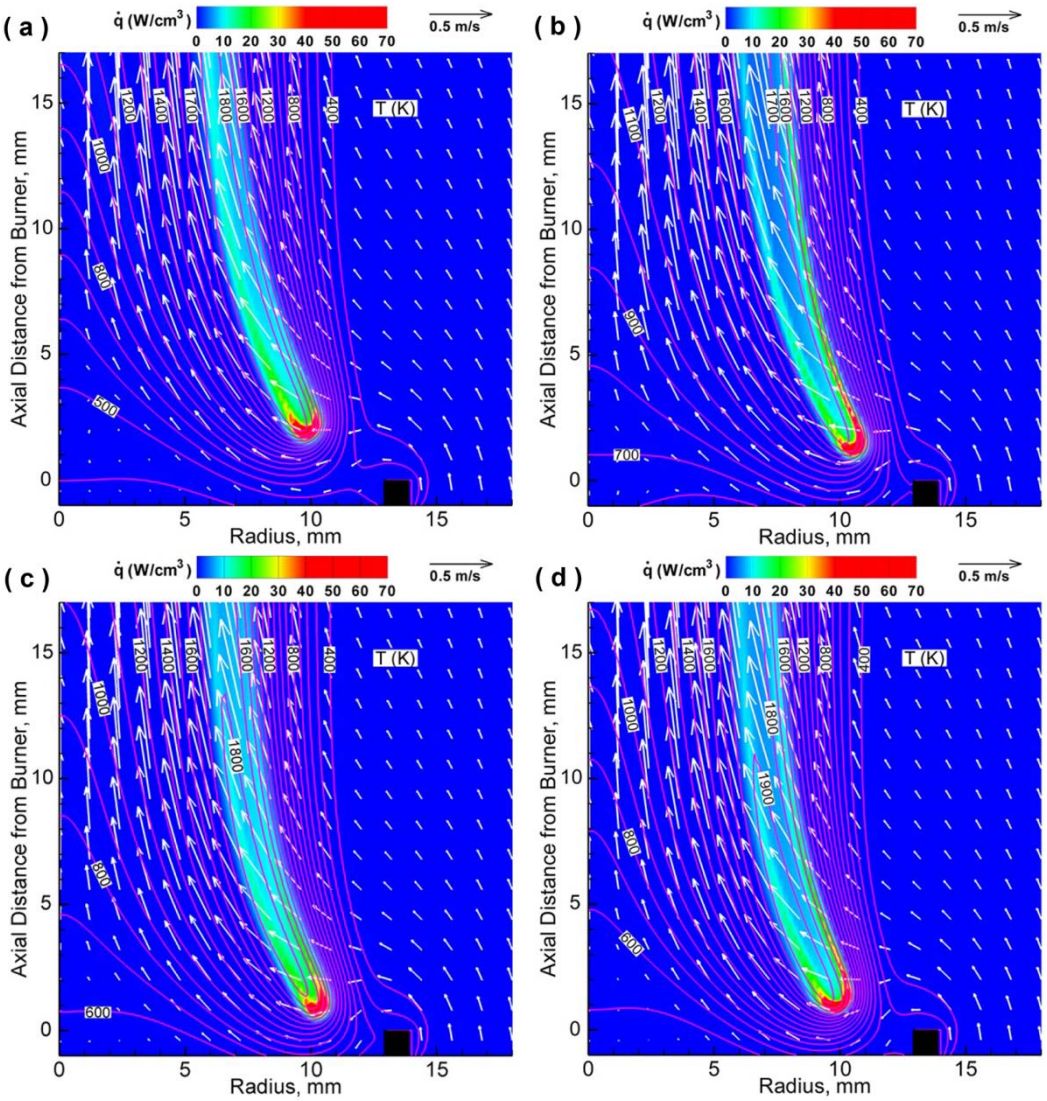

Figure 1. Calculated structure of near-limit propane flames in air with added agent: (a) CF_3Br, X_a=0.0258; (b) C_2HF_5, X_a=0.0765; (c) $C_2HF_3Cl_2$, X_a=0.0455; and (d) $C_3H_2F_3Br$, X_a=0.0246.

Unlike the flame with CF_3Br (Fig. 1a), the heat-release rate contours for the other near-limit flames, particularly with C_2HF_5 (Fig. 1b) and $C_3H_2F_3Br$ (Fig. 1d), show distinct "two-zone" flame structure.

Figure 2 shows the radial variations of the calculated temperature and heat-release rate in propane flames in air with agent: (a) across a trailing flame (z_k + 5 mm); (b) across the reaction kernel: z_k = 1.8 mm (CF_3Br), 1.2 mm (C_2HF_5), 0.8 mm ($C_2HF_3Cl_2$), and 1.4 mm ($C_3H_2F_3Br$). The trailing flames (Fig. 2a) are characterized by the two-zone flame structure (inner and outer) as evident from two heat-release rate peaks most prominently for C_2HF_5 and least significantly for CF_3Br. Although the temperature peak is closer to the inner reaction zone, formed by the hydrocarbon-O_2 combustion, the larger heat-release rate peak for C_2HF_5 is in the outer zone by highly exothermic reactions. The temperature and heat-release-rate profiles in the propane flame with C_2HF_5 (Fig. 2a) are similar to those obtained previously [7] for the ACT fuel with C_2HF_5.

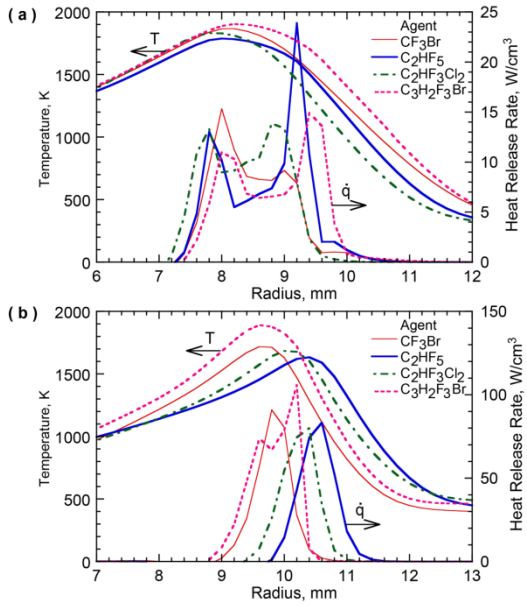

Figure 2. Calculated radial variations of the temperature and heat-release rate in propane flames in air with agent: (a) across a trailing flame (at z_k + 5 mm); (b) across the reaction kernel (at z_k). CF_3Br, X_a = 0.0258, z_k = 1.8 mm; C_2HF_5, X_a = 0.0765, z_k = 1.2 mm; $C_2HF_3Cl_2$, X_a = 0.0455, z_k = 0.8 mm; and $C_3H_2F_3Br$, X_a = 0.0246, z_k = 1.4 mm.

The outer heat-release-rate peak in the trailing flame in $1g_n$ (Fig. 2a) is more evident, compared to the $0g_n$ case [6], due to increased convective fluxes of reactants (i.e., the blowing effect [35]) by the buoyancy-induced incoming flow.

At the reaction kernel in the flame base region (Fig. 2b), the peak heat-release-rate for each agent slightly on the airside of each temperature peak is several times larger than that in the trailing flame. The peak temperature for $C_3H_2F_3Br$ is much higher than other agents, suggesting that additional number of carbon in the agent molecule, compared to CF_3Br, represent potential energy contributions at a fixed concentration.

Figure 3 shows the radial variations of the species volume fractions (X_i) crossing the trailing flame with C_2HF_5 (added at X_a=0.0765) at z= 6.2 mm. Oxygen penetrates through the outer zone and a pool of chain carrier radicals (H, O, and OH) is formed in the middle of the two zones at relatively high concentrations ($X_a \approx 10^{-3}$), thus contributing to both reaction zones. The initial hydrocarbon fuel (C_3H_8) diffuses from the fuel side, decomposes to fragments (CH_4, C_2H_4, and C_2H_2) and reacts with the chain carrier radicals in the inner zone. In the outer zone, the agent (C_2HF_5) from the air side decomposes to many fluorinated species (C_2F_6, CF_2, CHF_3, etc.), which react with the radicals. The H_2O (formed by hydrocarbon-O_2 reaction) diffuses to the outer zone, where it is converted to HF through highly exothermic reactions. The H_2O nearly vanishes in the outer zone in the propane flame, whereas that in the ACT fuel flame with C_2HF_5, reported previously [7], remains at a $X_a \approx 10^{-3}$ level even outside the outer zone due to its high content (X_{H2O} = 0.387) in the fuel. The CF_2O peak (X_{CF2O} = 0.031) in the outer zone in the propane flame is lower than that (X_{CF2O} = 0.048) in the ACT fuel flame. The final products (CO_2, HF, and CF_2O) are distributed radially in a wide range. Low levels of C_2HF_5 on the fuel side and H_2 on the air side in Fig. 3 are due to leakage in the opposite directions through the quenched zone below the flame base. These species' contributions to overall reactions in the opposite zones must be insignificant.

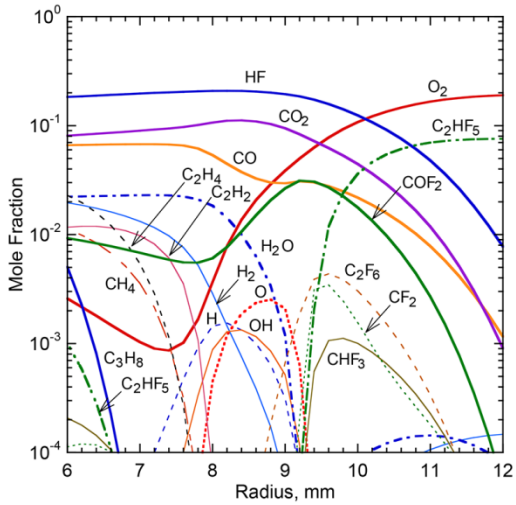

Figure 3. Calculated structure of a propane flame in air with added C_2HF_5 at X_a = 0.076 and z = 5.8 mm.

Figure 4 shows the radial variations of the calculated production (+) or consumption (-) rates (Fig. 4a) and heat-release rates (Fig. 4b) of species *i* crossing the trailing flame at z=5.8 mm in a propane flame in air with C_2HF_5 at X_a=0.076. In the inner zone, H_2, CO, and the chain carrier radicals (H, O, and OH) are formed and consumed, O_2, and CF_2O are consumed, and H_2O, HF and CO_2 are formed. In the outer zone, C_2HF_5 and O_2 are consumed and HF, CF_2O, and CO are formed. The major contributors to the overall heat-release rate (Fig. 4b) are the formation of H_2O, CO, CO_2 HF in the inner zone, with HF, CF_2O and CO in the outer zone. Although the production rates and heat-release rates of HF and CF_2O in the propane flame are significantly less than those in the ACT fuel flame [7], the resultant heat-release rate profiles are very similar for the two flames. The highly exothermic reactions with the heats of reactions in "( )" include:

$H_2 + OH \rightarrow H + H_2O$ (+61 kJ/mol) (R5)

$CO + OH \rightarrow CO_2 + H$ (+102 kJ/mol) (R61)

$H_2O + F \rightarrow OH + HF$ (+74 kJ/mol) (R1685)

$H_2 + F \rightarrow H + HF$(+135 kJ/mol) (R1679)

$CF_2 + OH \rightarrow CF_2O + H$ (+268 kJ/mol) (R1849)

$CF_3 + OH \rightarrow CF_2O + HF$ (+493 kJ/mol) (R1669)

$CF_2 + O \rightarrow CFO + F$ (+150 kJ/mol) (R1849)

$CF_3 + O \rightarrow CF_2O + F$ (+342 kJ/mol) (R1663)

$CF_3 + H \rightarrow CF_2 + HF$ (+215 kJ/mol) (R1719)

The reactions to form CF_2O are particularly exothermic because of its exceptionally low (negative) heat of formation (-640 kJ/mol).

Figure 5 shows the effects of the agent volume fraction in the coflowing oxidizer on the calculated axial (z_k) and radial (r_k) positions of the reaction kernel from the burner exit on the axis in propane flames. In the present unsteady calculations, as X_a was increased incrementally, the flame-stabilizing reaction kernel in the flame base detached from the burner rim and moved downstream (i.e., the inward and upward direction) gradually and then more steeply as the extinguishment limit approached. For each X_a, a stable stationary flame was obtained.

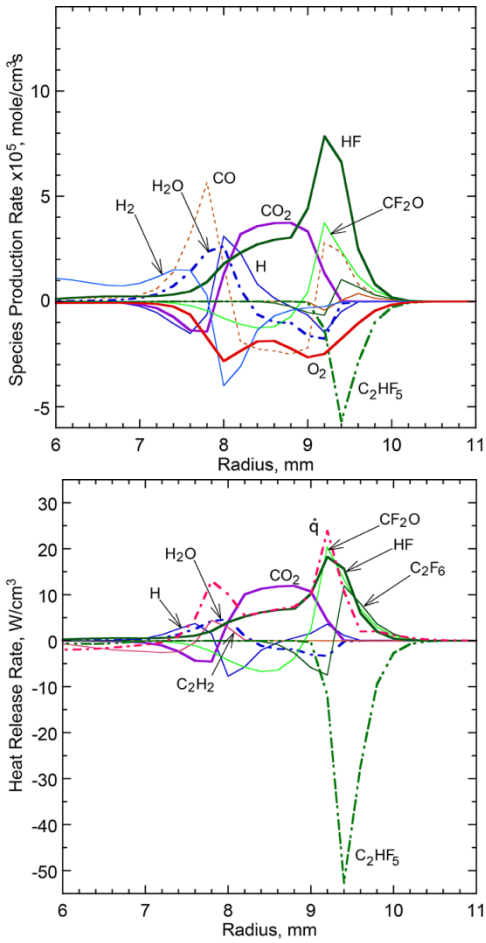

Figure 4. Calculated radial variations of the (a) species production rates, and (b) species and total heat-release rates in a propane flame in air with C_2HF_5 at X_a=0.076 and z=5.8 mm.

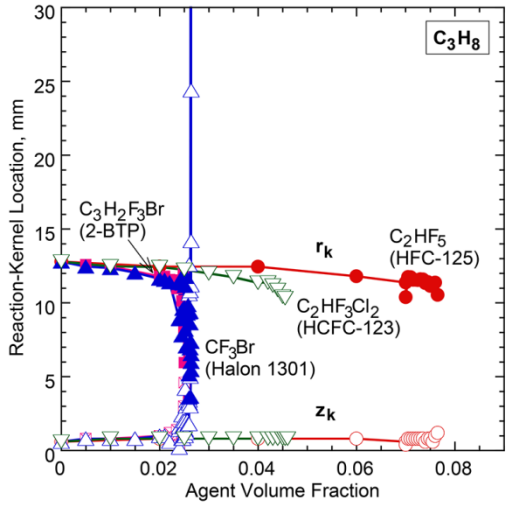

Figure 5. Calculated reaction kernel coordinates of propane flames in air with agent.

For CF_3Br (and, to a lesser extent, C_2HF_5), the flame base oscillated, until finally, blowoff-type extinguishment occurred, whereas for $C_2HF_3Cl_2$ and $C_3H_2F_3Br$, the calculation abruptly diverged at X_a=0.046 and X_a=0.025, respectively. The radial location of the reaction kernel decreased (inward) with X_a, thereby more premixing occurred over the standoff distance. For propane, the MECs of CF_3Br and C_2HF_5 (see Table 1) are: X_a ≈0.04 and ≈0.1, respectively (measured); and X_a=0.0264 and 0.0765, respectively (calculated). By considering technical difficulties, including the stiffness in the computation, complex combustion and inhibition chemistries, and transient blowoff phenomena with occasional flame-base oscillations, the calculated MECs are in fair agreement (≈30 %) with the measurements.

Figure 6 shows the maximum temperature in the trailing diffusion flame and the total heat-release rate ($\dot{q}_{\text{total}}$) integrated over the entire flame and over the flame base region ($\dot{q}_{<zk+3\text{ mm}}$). Thus, both the heat-release rate per unit volume along the flame and the flame size affect $\dot{q}_{\text{total}}$. Unlike chemically passive agents [37, 38], which work thermally to reduce the flame temperature by dilution, the maximum flame temperatures in the present work are nearly constant (≈1800 K) for C_2HF_5 or mildly increased for CF_3Br, $C_3H_2F_3Br$ and $C_2HF_3Cl_2$ as X_a increased until extinguishment. There is a striking difference in $\dot{q}_{\text{total}}$ over the entire flame between CF_3Br and the other agents: $\dot{q}_{\text{total}}$ decreased (i.e., inhibition) with added CF_3Br, whereas it increased (i.e., combustion enhancement) with C_2HF_5 or $C_2HF_3Cl_2$. It is neutral for $C_3H_2F_3Br$. In contrast, for all agents, $\dot{q}_{<zk+3\text{ mm}}$ was nearly constant as X_a increased. Thus, the combustion enhancement occurred only in the trailing flame. In fact, the heat release in the trailing flame ($\dot{q}_{\text{total}}$ - $\dot{q}_{<zk+3\text{ mm}}$) tripled with added C_2HF_5 (at X_a ≈0.08). This enhancement is ≈1.5x larger than the zero-gravity flames studied previously [6], because of much higher incoming flow velocity in normal gravity, resulting in higher reactants (agent and oxygen) influx into the flame zone. Although the volumetric heat-release rate in the trailing flame was an order-of-magnitude smaller than the peak $\dot{q}_k$, integration over the entire trailing flame zone made the total value much larger. This result suggests the significant implication that even if the reaction kernel, with *premixed*-like flame structure, is weakened by halogenated agent addition toward the flame stability limit, the trailing *diffusion* flame can burn more reactants (including the agent itself) because of the additional heat release to form HF and CF_2O in the aforementioned "two-zone" flame structure.

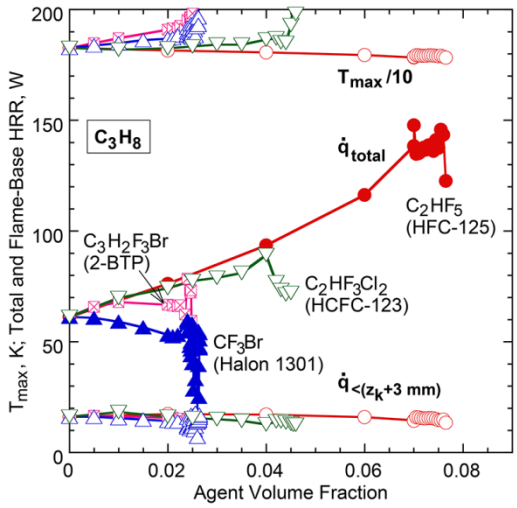

Figure 6. Calculated maximum temperature and total heat release rate (integrated over the entire flame and the base region) in propane flames in air with agent.

CONCLUSIONS

By using propane as the fuel, in addition to the ACT fuel studies previously, the physical and chemical effects of Halon 1301 (CF_3Br) and halon-replacement fire-extinguishing agents (C_2HF_5, $C_2HF_3Cl_2$, and $C_3H_2F_3Br$) are studied numerically to gain better understanding of the flame structure, combustion inhibition/enhancement, and blowoff extinguishment of cup-burner flames. Addition of agent to the coflowing air weakens the flame attachment point (reaction kernel) at the flame base, thereby inducing the detachment, lifting, and blowout extinguishment. With added agent, the calculated maximum flame temperature remains nearly constant (≈1800 K) for C_2HF_5 or mildly increases for CF_3Br, $C_3H_2F_3Br$, and $C_2HF_3Cl_2$. Moreover, the total heat release increases with agent addition for C_2HF_5 and $C_2HF_3Cl_2$ (by up to a factor of 2.5). In the trailing flame, H_2 and H_2O (from hydrocarbon combustion) are converted to HF and CF_2O by exothermic reactions, enhancing an inner flame zone, while reactions of the inhibitor, also forming of HF and CF_2O, created a large outer heat-release zone. In contrast, CF_3Br reduced the total heat release.

ACKNOWLEDGMENTS

This work was supported by The Boeing Company.

REFERENCES

1. Reinhardt, J.W., "Behavior of Bromotrifluoropropene and Pentafluoroethane When Subjected to a Simulated Aerosol Can Explosion," Federal Aviation Administration, DOT/FAA/AR-TN04/4, 2004.
2. Reinhardt, J.W., "Minimum Performance Standard for Aircraft Cargo Compartment Halon Replacement Fire Suppression Systems (2nd Update)," FAA, DOT/FAA/AR-TN05/20, 2005.
3. Linteris, G.T., Takahashi, F., Katta, V.R., Chelliah, H.K., and Meier, O., "Thermodynamic Analysis of Suppressant-Enhanced Overpressure in the FAA Aerosol Can Simulator," *Fire Safety Science – Proceedings of the Tenth International Symposium*, International Association for Fire Safety Science, Boston, MA, 2011, pp. 1-14.
4. Linteris, G.T., Burgess, D.R., Katta, V.R., Takahashi, F., Chelliah, H.K., and Meier, O., "Stirred Reactor Calculations to Understand Unwanted Combustion Enhancement by Potential Halon Replacements," Combustion and Flame 159: 1016-1025 (2012).
5. Linteris, G.T., Babushok, V.I., Sunderland, P.B., Takahashi, F., Katta, V.R., and Meier, O., "Unwanted Combustion Enhancement by $C_6F_{12}O$ fire Suppressant," Proc. Combust. Institute 34: 2683-2690 (2012).
6. Takahashi, F., Katta, V.R., Linteris, G.T., and Meier, O., "Cup-Burner Flame Structure and Extinguishment by C_2HF_5 in Microgravity," Proc. of the Combustion Institute 34: 2707-2717 (2012).
7. Takahashi, F., Katta, V.R., Linteris, G.T., and Babushok, V.I., "Combustion Inhibition and Enhancement of Cup-Burner Flames by CF_3Br, C_2HF_5, $C_2HF_3Cl_2$, and $C_3H_2F_3Br$," Proceedings of the Combustion Institute 35: 2741–2748 (2014).
8. Anon, "Standard on Clean Agent Fire Extinguishing Systems," National Fire Protection Association, NFPA 2001, Quincy, MA (2000).
9. Anon, Gaseous Fire-Extinguishing Systems Physical Properties and System Design, ISO 14520-Part I, International Organization for Standardization (2000).
10. Sheinson, R.S., Penner-Hahn, J.E., and Indritz, D., "The Physical and Chemical Action of Fire Suppressants," Fire Safety Journal 15: 437-450 (1989).
11. Hamins, A., Gmurczyk, G., Grosshandler, W., Rehwoldt, R.G., Vazquez, I., Cleary, T., Presser, C., and Seshadri, K., "Flame suppression effectiveness," in *Evaluation of Alternative In-Flight Fire Suppression for Full Scale Testing in Simulated Aircraft Engine Nacelles and Dry Bays* (W. Grosshandler, R. G. Gann, and W. M. Pitts, Eds.), NIST SP 861, pp. 345-465.
12. Linteris, G.T., "Flame Suppression Chemistry," in *Advanced Technology for Fire Suppression in Aircraft* (R. G. Gann, Ed.), NIST Special Publication 1069, pp. 119-338, 2007.
13. Linteris, G.T., "Acid Gas Production in Inhibited Propane-Air Diffusion Flames," in *Halon Replacements: Technology and Science* (A. W. Miziolek and W. Tsang, Eds.), American Chemical Society, Washington, DC, Chap. 19, pp. 225-242, 1995.

14. Linteris, G.T., Takahashi, F., and Katta, V.R., "Fuel Effects in Cup-Burner Flame Extinguishment," 5th US Combustion Meeting, San Diego, March 25-28, 2007.
15. Kim, A., "Overview of Recent Progress in Fire Suppression Technology," National Research Council of Canada, NRCC-45690, 2002.
16. Riches, J., Knutsen, L., Morrey, E., and Grant, K., "A Modified Flame Ionization Detector as a Screening Tool for Halon Alternatives," Halon Alternatives Technical Working Conference, Albuquerque, NM, pp. 115-125, 2000.
17. Grigg, J., Chattaway, A., and Ural, E.A, "Evaluation of Advanced Agent Working Group Agents by Kidde," Halon Options Technical working Conference, Albuquerque, NM, 2001.
18. Katta, V.R., Goss, L.P., and Roquemore, W.M., Numerical Investigations of Transitional H_2/N_2 Jet Diffusion Flames, AIAA Journal 32: 84-94 (1994).
19. Roquemore, W.M., and Katta, V.R., Role of Flow Visualization in the Development of UNICORN, Journal of Visualization 2: 3/4, 257-272 (2000).
20. Barlow, R.S., Karpetis, A.N., Frank, J.H., and Chen, J.-Y., "Scalar Profiles and NO Formation in Laminar Opposed-Flow Partially Premixed Methane/Air Flames," Combustion and Flame 127: 2102-2118 (2001).
21. Fuss, S.P., Hamins, A., "Determination of Planck Mean Absorption Coefficient for HBr, HCl and HF," Transaction ASME 124: 26–29 (2002).
22. Katta, V.R., Forlines, R.A., Roquemore, W.M., Anderson, W.S,. Zelina, J., Goad, J.R., Stouffer, S.D., Roy, S., "Experimental and Computational Study on Partially Premixed Flames in a Centerbody Burner," Combustion and Flame 158: 511-524 (2011).
23. Wang, H., You, X., Jucks, K.W., Davis, S.G., Laskin, A., Egolfopoulos, F., Law, C.K., "USC Mech Version II. High-Temperature Combustion Reaction Model of $H_2/CO/C_1$-C_4 Compounds," available at <http://ignis.usc.edu/USC_Mech_II.htm>, University of Southern California, Los Angeles, CA, 2007.
24. Sheen, D.A., You, X., Wang, H. and Lovas, T., "Spectral Uncertainty Quantification, Propagation and Optimization of a Detailed Kinetic Model for Ethylene Combustion," Proceedings of the Combustion Institute 32: 535–542 (2009).
25. Li, J., Kazakov, A., Chaos, M. , Dryer, F.L., "Chemical Kinetics of Ethanol Oxidation," US Sections/The Combustion Institute Meeting (2007).
26. Li, J., Kazakov, A., F.L. Dryer, "Ethanol pyrolysis experiments in a variable pressure flow reactor," Int. J. Chem. Kinetics 33: 859-867 (2001).
27. Babushok, V.I., Burgess, D.R.F., Tsang, W., and Miziolek, A.W., "Simulation Studies on the Effects of Flame Retardants on Combustion Processes in a Plug Reactor," In *Halon Replacements*, 1995, pp. 275-288.
28. Babushok, V.I., Noto, T., Burgess, D.R.F., Hamins, A., and Tsang, W., "Influence of CF_3I, CF_3Br, and CF_3H on the High-Temperature Combustion of Methane," Combustion and Flame 107: 351-367 (1996).
29. Babushok, V.I., Linteris, G.T., Meier, O.C., and Pagliaro, J.L., Combustion Science and Technology (2014), in press.
30. Pagliaro, J.L., Babushok, V.I., and Linteris, G. T., Combust. Flame (2014), in press.
31. Burgess, D.R., Zachariah, M.R., Tsang, W., and Westmoreland, P.R., "Thermochemical and Chemical Kinetic Data for Fluorinated Hydrocarbons," Progress in Energy and Combust. Sci. 21: 453-529 (1995).
32. Burgess, D., Zachariah, M.R., Tsang, W., and Westmoreland, P.R., "Thermochemical and Chemical Kinetic Data for Fluorinated Hydrocarbons," NIST Technical Note 1412, National Institute of Standards and Technology, Gaithersburg, MD, 1995.
33. Zegers, E.J.P., Williams, B.A., Fisher, E.M., Fleming, J.W., and Sheinson, R.S., "Suppression of Nonpremixed Flames by Fluorinated Ethanes and Propanes," Combust. Flame 121: 471-487 (2000).
34. Takahashi, F., and Katta, V.R., "A Reaction Kernel Hypothesis for the Stability Limit of Methane Jet Diffusion Flames," Proceedings of the Combustion Institute 28: 2071-2078 (2000).
35. Takahashi, F., Linteris, G.T., and Katta, V.R., "Vortex-Coupled Oscillations of Edge Diffusion Flames in Coflowing Air with Dilution," Proceedings of the Combustion Institute 31: 1575-1582 (2007).
36. Takahashi, F., Linteris, G.T., and Katta, V.R., "Extinguishment of Methane Diffusion Flames by Carbon Dioxide in Coflow Air and Oxygen-Enriched Microgravity Environments," Combustion and Flame 155: 37-53 (2008).
37. Takahashi, F., Linteris, G.T., and Katta, V.R., "Extinguishment of Methane Diffusion Flames by Inert Gases in Coflow Air and Oxygen-Enriched Microgravity Environments," Proceedings of the Combustion Institute:33: 2531-2538 (2010).